Nanotechnology

Manipulation of Gold Nanoparticles inside Transparent Materials**

Jianrong Qiu, Xiongwei Jiang, Congshan Zhu, Mitsuru Shirai, Jinhai Si, Nan Jiang, and Kazuyuki Hirao*

Nanoparticles have a wide range of electrical and optical properties owing to the quantum-size effect, surface effect, and conjoint effect of nanostructures.[1] Materials doped with noble-metal nanoparticles exhibit large third-order nonlinear

[*] Prof. J. Qiu, X. Jiang, Prof. C. Zhu
Photon Craft Project
Shanghai Institute of Optics and Fine Mechanics
Chinese Academy of Sciences and
Japan Science and Technology Corporation
Shanghai 201800 (China)
Fax: (+86) 21-5992-9373
E-mail: jrq@photon.jst.go.jp

M. Shirai, J. Si
Photon Craft Project
Japan Science and Technology Corporation
SuperLab 205
Keihanna-Plaza, Kyoto 619-0237 (Japan)

N. Jiang
Department of Physics and Astronomy
Arizona State University
Tempe, AZ 85287 (USA)

Prof. K. Hirao
Department of Material Chemistry
Graduate School of Engineering
Kyoto University
Sakyo-ku, Kyoto 606-8501 (Japan)

[**] J.Q. acknowledges support from the National Natural Science Foundation of China (No:50125208). We thank Mr. T. Nakaya (JST, Kyoto) and Prof. P. Kazansky (Southampton Univ. (UK)) for helpful discussions.

  DOI: 10.1002/ange.200352380

susceptibility and ultrafast nonlinear responses.[2] They are expected to be promising materials for ultrafast all-optical switches in the THz region. For the applications related to integrated optoelectronics, a well-defined assembly and spatial distribution of nanoparticles in materials are essential.[3] Many studies have been carried out on the fabrication of nanoparticle-doped materials,[4] but there are no effective methods to control the spatial distribution of nanoparticles in these materials. In addition, Zheng and Dickson reported the synthesis of photostable, water-soluble, silver nanodots by direct photoreduction of silver ions under ambient conditions.[5] Photoactivated fluorescence has also been observed from individual silver nanoclusters.[6] Herein, we report a method that can control the precipitation of Au nanoparticles in three dimensions inside transparent materials by using focused femtosecond laser irradiation. In brief, the precipitation involves two processes: the photoreduction of Au ions to atoms induced by multiphoton process, and the precipitation of Au particles driven by heat treatment. The size of nanoparticles and their spatial distribution can be controlled by the conditions of the laser irradiation. Interestingly, the precipitated nanoparticles obtained by this technique can be also space-selectively "dissolved" by the femtosecond laser irradiation, and reprecipitated by annealing. This implies that the laser can be used not only in practical applications, such as the 3D optical memory and the fabrication of integrated all-optical switches, but also in the study of the control of nucleation and crystal growth.

Au_2O_3-doped (0.01 mol%) silicate glass samples were irradiated by using a focused Ti–sapphire mode-locked femtosecond laser beam (800 nm, 120 fs, 1 KHz) with an intensity of $3.5 \times 10^{15}\ W\,cm^{-2}$ for 1/63 s (16 laser pulses) on each spot. Gray spots of about 40 μm in diameter were then observed in the focused area through an optical microscope after irradiation. No microcracks were observed in the samples. After the samples were annealed at 550 °C for 30 min, the gray spots became red. Using this technique, we first drew a gray owl with the laser beam, and then annealed the sample at 550 °C for 30 min, and as expected, the gray owl became red. After the sample cooled down to room temperature, we drew a gray butterfly in a different area of the sample. These images are shown in Figure 1.

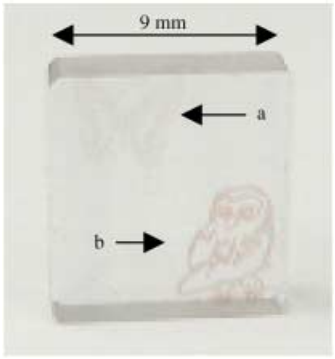

Figure 1. Photograph of images drawn inside the Au_2O_3-doped glass (0.01 mol%) by using the femtosecond laser irradiation: a) gray butterfly (without annealing); b) red owl (with annealing).

Figure 2 shows extinction spectra of the Au_2O_3-doped glass sample before and after femtosecond laser irradiation. There is an apparent increase in extinction in the wavelength region from 300 to 800 nm in the irradiated area. The inset of the Figure 2 shows the difference extinction spectrum of the glass sample before and after the laser irradiation. The peaks at 245, 306, 430, and 620 nm can be assigned to E′ centers (E′ = Si), which include an electron trapped in an sp^3 orbital of silicon at the site of an oxygen vacancy, a hole trapped by an oxygen vacancy that neighbors alkali-metal ions, and nonbridging oxygen holes HC1 (a hole trapped by an SiO_4 polyhedron that contain one bridging oxygen and three nonbridging oxygen atoms) and HC2 (a hole trapped by an SiO_4 polyhedron that contain two nonbridging oxygen atoms).[7]

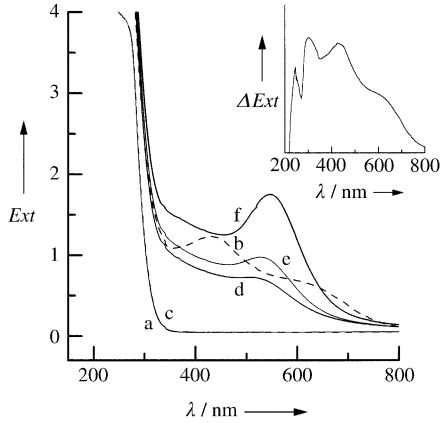

Figure 2. Extinction spectra of the Au_2O_3-doped glass (0.01 mol%). a) Before femtosecond laser irradiation; b) after femtosecond laser irradiation; c), d), e), and f) after femtosecond laser irradiation and subsequent annealing at 300, 450, 500, and 550 °C for 30 min, respectively. Inset of Figure 2. Difference extinction spectrum of the Au_2O_3-doped glass sample (0.01 mol%) before and after the femtosecond laser irradiation.

The extinction spectra of the Au_2O_3-doped glasses, which were annealed at various temperatures for 30 min after irradiation, are also plotted in Figure 2. When the annealing temperature is below 300 °C, the extinction (300–800 nm) intensities induced by irradiation decrease as the annealing temperature increases, and completely disappear when the temperatures reaches 300 °C. One can see in Figure 2 that spectrum a and c are almost identical. The gray induced by the femtosecond laser irradiation disappears at 300 °C and the glass becomes colorless and transparent. Annealing at 450 °C results in the appearance of a new peak at 506 nm, and the laser-irradiated areas turn red. The extinction peak can be assigned to the surface plasmon resonance absorption of Au nanoparticles.[2] The wavelength of the extinction peak increases from 506 to 526 to 548 nm with increasing annealing temperature, at the same time its intensity significantly increases. Based on the Mie theory, $R \propto \lambda_p^2/\Delta\lambda$, in which R is the average radii of the metal nanoparticles, λ_p is the characteristic wavelength of surface plasmon resonance and $\Delta\lambda$ is the full width at half maximum of the absorption band.[8]

The value of $\lambda_p^2/\Delta\lambda$ increases from 1306 to 1774 to 2208 nm when the annealing temperature is increased from 450 to 500 to 550 °C. Therefore, the average size of the Au nanoparticles increases with increasing annealing temperature.

Figure 3 is a TEM image showing the precipitation of nanoparticles in the laser-irradiated Au_2O_3-doped glass after annealing at 550 °C for 30 min. Composition analysis by using energy dispersive spectroscopy (EDS) in TEM confirms that these spherical nanoparticles are metallic Au. The size of the Au nanoparticles ranges from 6 to 8 nm.

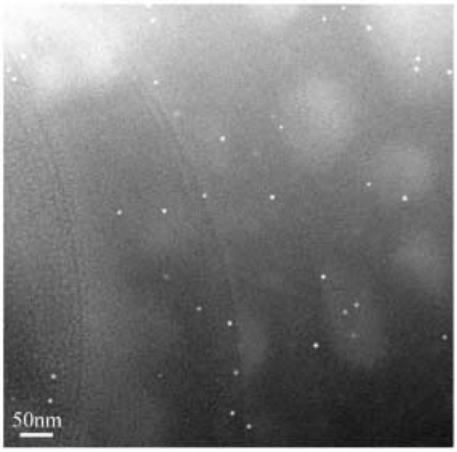

Figure 3. TEM image of Au nanoparticles (small white dots) in the laser-irradiated Au_2O_3-doped (0.01 mol%) glass after annealing at 550 °C for 30 min.

The inset of Figure 4 shows the photograph of a Au_2O_3-doped glass sample, which is irradiated by using femtosecond laser beams of 6.5×10^{13}, 2.3×10^{14}, or 5.0×10^{16} W cm^{-2} in the different areas and then annealed at 550 °C for 1 hour. With increasing light intensity, the color of the laser-irradiated areas became violet, red, or yellow. Figure 4 shows the extinction spectra from these different colored areas. The extinction peak shifts from 568 to 534 to 422 nm with the increase of the light intensity. The peak with the wavelength longer than 500 nm observed at spectra a and b, can also be assigned to the surface plasmon resonance absorption of the Au nanoparticles. The apparent blue shift of the peak from 568 to 534 nm is due to the decrease in the average size of the Au nanoparticles. An extinction peak is observed at 420 nm (2.94 eV) in the spectrum c of the Figure 4. There are few reports on the observation of such peaks in glasses doped with Au nanoparticles. However, the peak position and shape are very similar to those of an undecagold compound with small Au clusters, for example, $[Au_{11}]$.[9] The peak can be attributed to interband transitions from 5d to 6sp, that is, originating in the submerged and quasicontinum 5d band and terminating in the lowest unoccupied conduction band of the Au clusters. The average size of Au nanoparticles in area c (Figure 4 inset) is much smaller than those in areas a and b. Therefore, the average size of the Au nanoparticles decreases with an increase of the light intensity. This is probably because the high irradiation intensity produces a high concentration of reduced Au atoms per unit volume, and thus a high concentration of nucleation centers. As a result, under the same annealing process, the higher the light intensity, the smaller but denser the precipitated particles are. Further investigation is needed to verify the above hypothesis.

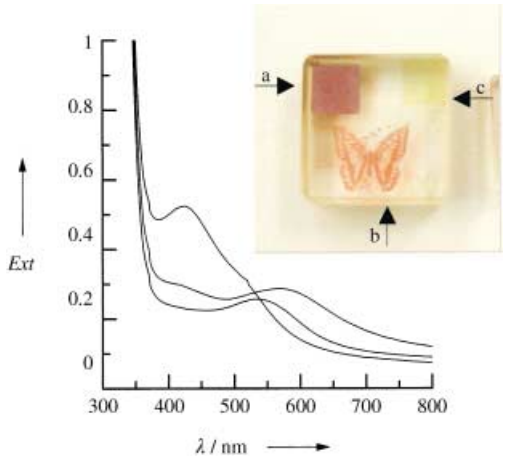

Figure 4. Extinction spectra of Au_2O_3-doped glasses (0.1 mol%) irradiated by using different light intensities: a) 6.5×10^{13} W cm^{-2}; b) 2.3×10^{14}; c) 5.0×10^{16}. All samples were annealed at 550 °C for 1 hour. Inset of Figure 4: Photograph of images drawn inside the Au_2O_3-doped (0.1 mol%) glass sample.

The reduction of Au ions to atoms by femtosecond laser irradiation is the key process of this method. Au ions capture the "free" electrons created by multiphoton processes and are then reduced to atoms, which aggregate to form nanoparticles during annealing. A similar phenomena have also been observed with Ag^+ ions that have been irradiated with X-rays.[4] To test this mechanism, we studied the white emission observed during the femtosecond laser irradiation. If the light intensity was sufficiently high and the laser beam was not tightly focused, supercontinuum white light due to the self-phase modulation of the laser beam was observed during the laser irradiation. We observed that the gray area was induced in the area where supercontinuum white light was observed in the glass. We tightly focused the laser beam and confirmed that the gray area was generated in the area at which white emission was observed, even when no supercontinuum was detected. The white emission is due to plasma formation.[10] It was also found that three areas, the white emission area, the gray area, and the nanoparticle-precipitated area were basically the same. If the diameter of the beam was kept the same (9 μm), the length of emission region was proportional to the light intensity, which increased from 1.2×10^{14} to 4.0×10^{15} W cm^{-2}. In general, the light intensity, in order of 10^{14}–10^{17} W cm^{-2}, is high enough to generate multiphoton ionization in the glass matrix.[10] Therefore, the active electrons and holes can be created in the glass through multiphoton ionization, Joule heating, and collisional ionization,[10] and form plasma, which yield white emission. Electrons are driven out of the valence states by multiphoton absorption of the incident photon. Some of the Au ions capture free electrons to form Au atoms. At temperatures below 300 °C, only some trapped electrons and holes are excited by thermal energy and recombine with each other. When annealing at temperatures

above 400 °C, Au atoms get sufficient energy to overcome the interaction between the Au atoms and the glass network structure and start to move. The formation of the Au nanoparticles is due to the aggregation of Au atoms. It is also confirmed that no change occurs in the extinction spectrum of the nanoparticle-precipitated glass sample at room temperature, even over a period of six months. This indicates that the precipitated nanoparticles are stable at room temperature. Additionally, the precipitation of Au nanoparticles was not seen in the glass sample without laser irradiation, even after the sample had been annealed at 600 °C for more than 2 h. Therefore, the reduction of an Au ion to an atom by femtosecond laser irradiation is essential in forming Au nanoparticles, and the Au atom acts as a crystal nucleus for crystal growth.

Figure 5 shows the changes of the Au nanoparticle-precipitated Au_2O_3-doped glass sample after further laser

Figure 5. Photographs of images drawn inside the Au_2O_3-doped glass (0.01 mol%): a) by using femtosecond laser irradiation and annealing at 550 °C for 30 min; b) further irradiation at the center part of the image in (a) by focused femtosecond laser by using a 20× objective lens; c) then the glass was annealed at 300 °C for 300 min.

irradiation. The glass sample was first irradiated by the focused laser with a light intensity of 5.8×10^{14} W cm^{-2} and a scanning rate of 1000 μm s^{-1}, and then it was annealed at 550 °C for 30 min. The laser-irradiated area became red as shown in Figure 5a, as discussed above. Then the laser beam was focused on the center of the region where the nanoparticles had been precipitated and lines were drawn with the laser that were slightly longer than the nanoparticle region (Figure 5b). The light intensity and scanning rate were 3.9×10^{14} W cm^{-2} and 1000 μm s^{-1}, respectively. One can see that there is a slight change between Figure 5a and b due to the formation of colored centers. After the annealing process at 300 °C for 30 min, the second femtosecond laser-irradiated part became transparent, which is shown in Figure 5c. Interestingly, the transparent part in the center became red after further annealing of the sample at 550 °C for 30 min. Figure 6 shows the extinction difference between the sample before (Figure 5a) and after (Figure 5b) the second laser irradiation. It is clear that the extinction due to the surface plasmon resonance absorption decreases while the absorption due to the nonbridging oxygen hole centers HC1(430 nm) and HC2 (620 nm) increases after further laser irradiation. Therefore, we suggest that some of the nanoparticles are broken into small-size particles or atoms owing to the strong interaction between the Au nanoparticles and ultrashort laser pulses such as dramatic heating of nanoparticles due to

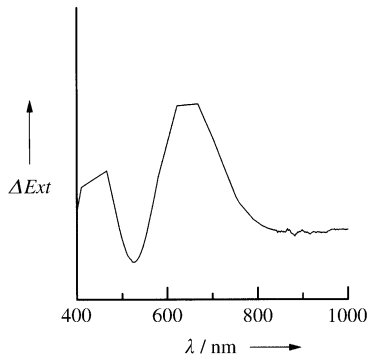

Figure 6. Spectrum showing the difference in extinction between nanoparticle sample before (Figure 5a) and after (Figure 5b) the second laser irradiation.

the linear and nonlinear absorption of laser energy during the further femtosecond laser irradiation.

Many experiments have confirmed that it is possible to control the diameter and longitudinal spread of the structurally changed area from several hundred nanometers to several millimeters by selecting the appropriate irradiation conditions, such as light intensity and diameter of the laser beam.[11] Our results further prove that it is also possible to precipitate Au nanoparticles in such microscopic dimensions inside materials by using the focused nonresonant femtosecond pulsed laser and successive annealing. The 3D gray images created by the laser can be erased after annealing at a lower temperature, and can be turned into various colors by annealing at higher temperatures. Therefore, this present technique will be useful in the fabrication of 3D multicolored industrial art objects, optical memory with ultrahigh storage density and ultrahigh recording speed, and integrated waveguide all-optical switches with ultrafast nonlinear responses. By using an Ag^+ ion-doped photosensitive glass, we have space-selectively precipitated silicate crystals inside the glass.[12] We believe it will be possible to spatially control the growth of other functional crystals in glasses. Recently, we have also succeeded in the fabrication of a grating of 400 nm in width by precipitating Au nanoparticles. Owing to the extremely short energy-deposition time and elimination of the thermal effect and nonlinear processes enabled by highly localizing laser photons in both time and spatial domains, the size of the laser-induced microstructures may be less than the diffraction limit. [13] In glasses with a high concentration of Au ions, we expect to able to produce 3D Au nanocircuits.

Experimental Section

The silicate glasses used in this study were $70SiO_2 \cdot 10CaO \cdot 20Na_2O$ (mol%) doped with different concentration of Au_2O_3. Reagent grade SiO_2, $CaCO_3$, Na_2CO_3, and $AuCl_3 \cdot HCl \cdot 4H_2O$ were used as starting materials. Approximately 40 g batches were mixed and melted in platinum crucibles in an electronic furnace at 1550 °C for 1 hour under the ambient atmosphere. The melts were then quenched to room temperature to obtain transparent and colorless glasses. The glass samples were cut and polished to sizes of $3 \times 9 \times 9$ mm^3 or $4 \times 10 \times 10$ mm^3, then were used in our experiments.

A Ti sapphire laser system with an oscillator (Tsunami pumped by a solid-state laser Millennia, both from Spectra Physics Co. Ltd.) and an amplifier (Spitfire pumped by Merlin both from Spectra Physics Co. Ltd.) was used in this study. The system emits 800 nm, 120 fs laser pulses at a 1 kHz repetition rate. To write an image inside the glass sample, the laser beam was focused by a 10× objective lens with an aperture of 0.30 onto the interior of the glass, about 1 mm beneath the surface. The glass sample was put on a computer-controlled *XYZ* stage. The diameter of the laser beam was 9 μm. Extinction spectra were acquired with a spectrophotometer (JASCO V-570). The size and composition of precipitated nanoparticles were examined in a JEOL-2010FEF transmission electron microscope (TEM) equipped with energy dispersive X-ray spectrometer (EDS) operating at an accelerating voltage of 200 kV.

Received: July 18, 2003
Revised: January 19, 2004 [Z52380]
Published Online: January 19, 2004

Keywords: glass · gold · laser chemistry · nanostructures · reduction

[1] A. P. Alivisatos, *Science* **1996**, *271*, 933 – 937.
[2] H. Inouye, K. Tanaka, I. Tanahashi, K. Hirao, *Phys. Rev. B* **1998**, 57, 234 – 240.
[3] B. Q. Wei, R. Vajtai, Y. Jung, J. Ward, R. Zhang, G. Ramanath, P. M. Ajayan, *Nature* **2002**, *416*, 495 – 496; Y. A. Vlasov, X. Z. Bo, J. C. Sturm, D. J. Norris, *Nature* **2001**, *414*, 289 – 292; Y. Huang, X. Duan, Q. Wei, C. M. Lieber, *Science* **2001**, *291*, 630 – 633.
[4] W. H. Armistead, S. D. Stookey, *Science* **1964**, *144*, 150 – 154; E. Valentin, H. Bernas, C. Ricolleau, F. Creuzet, *Phys. Rev. Lett.* **2001**, *86*, 99 – 102; H. Homfmeister, S. Thiel, M. Dubiel, E. Schurig, *Appl. Phys. Lett.* **1997**, *70*, 1694 – 1696.
[5] J. Zheng, R. M. Dickson, *J. Am. Chem. Soc.* **2002**, *124*, 13982 – 13983.
[6] L. A. Peyser, A. E. Vinson, A. P. Bartko, R. M. Dickson, *Science* **2001**, *291*, 103 – 106.
[7] A. Bishay, *J. Non-Cryst. Solids* **1970**, *3*, 54 – 114.
[8] G. Mie, *Ann. Phys.* **1908**, 25, 377 – 445; D. Manikandan, S. Mohan, P. Magudapathy, K. G. M. Nair, *Phys. B* **2003**, *325*, 86 – 91.
[9] E. Gutierrez, R. D. Powell, F. R. Furuya, J. F. Hainfeld, T. G. Schaaff, M. N. Shafigullin, P. W. Stephens, R. L. Whetten, *Eur. Phys. J. D* **1999**, *2*, 647 – 651.
[10] B. C. Stuart, M. D. Feit, A. M. Rubenchik, B. M. Shore, M. D. Perry, *Phys. Rev. Lett.* **1995**, *74*, 2248- 2251.
[11] K. M. Davis, K. Miura, N. Sugimoto, K. Hirao, *Opt. Lett.* **1996**, *21*, 1729 – 1731; E. N. Glezer, M. Milosavljevic, L. Huang, R. J. Finlay, T.-H. Her, J. P. Callan, E. Mazur, *Opt. Lett.* **1996**, *21*, 2023 – 2025; K. Miura, J. Qiu, H. Inouye, T. Mitsuyu, K. Hirao, *Appl. Phys. Lett.* **1997**, *71*, 3329 – 3331; E. N. Glezer, E. Mazur, *Appl. Phys. Lett.* **1997**, *71*, 882 – 884; J. Qiu, C. Zhu, T. Nakaya, J. Si, F. Ogura, K. Kojima, K. Hirao, *Appl. Phys. Lett.* **2001**, *79*, 3567 – 3569; H. Sun, Y. Xu, S. Joudkazis, K. Sun, M. Watanabe, J. Nishii, S. Matsuo, H. Misawa, *Opt. Lett.* **2001**, *20*, 325 – 327.
[12] Y. Kondo, J. Qiu, T. Mitsuyu, K. Hirao, T. Yoko, *Jpn. J. Appl. Phys.* **1999**, *38*, L1146 – 1148.
[13] K. Miura, J. Qiu, S. Fujiwara, S. Sakaguchi, K. Hirao, *Appl. Phys. Lett.* **2002**, *80*, 2263 – 2265.

